



EFFICIENCY OF USING CFRP COVERED AREA RATIO ON BEAM SHEAR CAPACITY

A. M. Abu-bakr*, S.A. Elbatal, M. M. Abo-Alanwar

Civil Engineering Department, Faculty of Engineering, Al-Azhar University, Nasr City, 11884, Cairo, Egypt,

*Correspondence: engahmedabubakr92@gmail.com

Citation:

Abu-bakr,A.M, Elbatal, S.A. and Abo-Alanwar, M.M. " Effect of cover area ratio with variables shear spans on beam shear capacity using carbon fiber", Journal of Al-Azhar University Engineering Sector, vol. 20, pp. 32 - 58, 2025

Received: 17 November 2024

Revised: 19 December 2024

Accepted: 06 January 2024

Doi: 10.21608/aej.2025.337128.1736

Copyright © 2025 by the authors. This article is an open-access article distributed under the terms and conditions of Creative Commons Attribution-Share Alike 4.0 International Public License (CC BY-SA 4.0)

ABSTRACT

Shear failure is a critical concern in reinforced concrete structures. Failure occurs suddenly without any warning. This study investigated a comprehensive finite element modelling using the ANSYS (V17.0) software approach to assess carbon fiber (CFRP) efficiency for RC beams. The dimensions of RC-supported beams were 120 mm in width and 400 mm in thickness. Four different length-to-thickness ratios, 3, 4, 5 and 6 have been considered. The different covered area of CFRP was applied to the RC beam to improve beam shear capacity. Four different percentages of CFRP, 12.5%, 25%, 37.5% and 50% related to effective shear zone area have been studied. CFRP was wrapped around the beam in a U-shape with anchors. Vertical deflection, failure load, von Mises stress and stress in the stirrups have been obtained. The analysis of results showed that the use of CFRP significantly improves the ductility and performance of RC beams. CFRP strengthening can shift the failure mode from shear to flexure, especially in beams with longer shear spans. This failure occurs in the flexure zone due to compression in the concrete, allowing it to undergo larger deformations before failure. Increasing the CFRP coverage from 12.5% to 50% for beams with an L/T ratio of 3 to 6 leads to an improvement in shear capacity ranging from 21.2% to 150%.

KEYWORDS: RC beam, Shear strengthen, Carbon fiber, Anchors, Finite element analysis, Ansys.

كفاءة استخدام ألياف الكربون بمساحات نسبية على قدرة مقاومة القص للكمرات

أحمد ابو بكر محمد*، سامح البطل عبد الحليم، محمد أبو الانوار محمود

قسم الهندسة المدنية، كلية الهندسة، جامعة الأزهر، مدينة نصر، 11884، القاهرة، مصر
*البريد الإلكتروني للباحث الرئيسي: engahmedabubakr92@gmail.com

الملخص

تقدم هذه الدراسة مجموعة من تقنيات نمذجة العناصر المحدودة لفحص فعالية التقنيات المختلفة في تقوية الكمرات الخرسانية ضد فشل القص. يعد فشل القص مشكلة كبيرة في الهياكل الخرسانية المسلحة، حيث يحدث بشكل غير متوقع ودون سابق انذار. تم استخدام تقنية تغطية ألياف الكربون بنسب مختلفة حول ثلاثة أوجه من الكمرات الخرسانية (الجانبية والسفلية) بحيث يتم استخدام مسامير لتثبيت الشرائح وتم دراسة سلوك الكمرات لمختلف نسب التغطية 12.5% و 24% و 37.5% و 50% من مسطح القص الإجمالي، كما تم دراسة سلوك مختلف النسب لأكثر من نسبة طول الي عمق الكمرات لاربع قيم متتالية 3، 4، 5 و 6 مرات عمق الكمرات الإجمالي ودراسة تأثير نسب التغطية لكلا منهم. تم الحصول على قيم الإزاحة الرأسية، حمل الفشل، إجهاد فون ميزيس للكمرات، وإجهادات الكانات الداخلية. أظهرت نتائج التحليل أن استخدام ألياف الكربون يُحسن بشكل كبير من اللدونة والأداء للكمرات الخرسانية المسلحة. يمكن أن يؤدي تعزيز الكمرات باستخدام ألياف الكربون إلى تغيير نمط الفشل من القص إلى الانحناء، خاصة في الكمرات ذات المسافات بين الدعامات الطويلة. يحدث الفشل في منطقة الانحناء بسبب الضغط في الخرسانة،

مما يسمح للكمرات الخرسانية المسلحة بالتحمل والانبعاج بشكل أكبر قبل الوصول إلى الفشل. إن زيادة تغطية ألياف الكربون من 12.5% إلى 50% للكمرات التي تتراوح بها نسبة النخافة (الطول الي العمق الاجمالي) من 3 إلى 6 يؤدي إلى تحسين في قدرة التحمل على القص تتراوح نسبته بين 21.2% و 150%.

الكلمات المفتاحية: الكمرات الخرسانية، مقاومة القص، ألياف الكربون فايبر، المسامير، تحليل العناصر المحدودة.

1. INTRODUCTION

Strengthening of reinforced concrete members, particularly beams and columns, is crucial. Strengthening means upgrading the strength of a structure by increasing its. Most of the work that was carried out was focused on the repair and strengthening of R.C. elements using steel angles, steel plates and/or R.C. jackets. A new strengthening method by using fiber-reinforced polymers FRP in strengthening reinforced concrete elements has been used recently. The following literature reviews for strengthening and repairing reinforced concrete beams especially. Abdel-Halim and Schorn [1] studied the effect of removing the cover concrete and recovering it. The results indicated that this gave more strength, the shotcrete layers and parent concrete remained bonded and acted together throughout loading until failure. Chajes and Thomson and Finch [2] compared E-glass and graphite fabrics to evaluate stiffness and strengths. It was seen that the compared to control beams with only internal steel, E-glass and graphite fabrics shown increased capacities of 53.2% and 45.6% respectively. Garden and Quantrill and Hollaway [3] evaluated the behavior of bonded CFRP plates, they found that the stiffening impact is greatest when the member's initial stiffness has been considerably reduced. This increases the beam stiffness most beyond the yield of the internal reinforcement. This illustrates how bonding plates can be applied to a severely damaged structure. Abdel-Jaber and Walker and Hutchinson [4] strengthened RC-beams against shear failure using externally bonded carbon fibre, bonding CFRP plates along the whole depth of the shear span results in the largest achieve in shear strength (up to 122% for the tested beams). Strips are less effective than CFRP plates over the full shear span, and the process is probably going to be costly. Zhang and Moren [5] investigated a U-shaped CFRP wrapping with anchorage to enhance shear capacity. The great increase in shear capacity was achieved by using a U-shaped CFRP wrapping with anchorage. Thakeb and El Sebai and El Esnawi and Amer [6] reviewed the behavior of clamps to steel plates or steel angles on the mode of failure. Provided clamps to steel plates or steel angles lead to changes in the mode of failure from shear to flexure mode. Tanarslan and Ertutar [7] investigated the effect of shape and orientation of CFRP strips on beam shear capacity. The side shape, L shape, and U-jacket are taken into consideration. The ultimate shear capacity of the U-jacketed specimen was 90 kN, which is 127% greater than that of the control beam. Additionally, the U-jacketed specimen had a 65% greater ultimate shear capacity than the L-shaped one. Consequently, it was established that the best strengthening method for the shear strengthening was U-jacketing. Debonding caused side-bonded and U-jacketed specimen beams without anchorage to collapse with brittle shear failure. One of the primary issues with CFRP-strengthened RC constructions is this. In order to prevent brittle shear failure due to early debonding, a new anchorage detail was created in the experimental program. The anchorage detail worked well. Amer and Mohammed [8] Compare the efficiency of using CFRP and GFRB for shear strengthening. The results indicated that the CFRP is more efficient than GFRP in shear strengthening of the reinforced concrete beams. Tanarslan [9] investigated the impact CFRP behaviour on the stiffness of the R.C beam. According to the test results, the CFRP improved the

specimen's strength; however, when the specimen was subjected to greater loads, more cracks appeared at the shear span, which decreased the stiffness in comparison to the control beam. Test results indicate that CFRP reinforcements are unable to raise the specimens' intended level of stiffness. VijayKumar and Venkatesh and Jayaprakash [10] studied behaviour of FRP reinforcement on the mode of failure. The results showed that using FRP shifted the behaviors of the control beams from shear failure near the ends of the beam to flexure failure at the mid-span of the beams. Jayajothi and kumutha and vijai [11] strengthened using a single layer with a U-wrapped CFRP and compared it with the control beam. It was found to have a higher shear capacity when compared with the control beam. Jayalin and Prince and karthika [12] compared the performance of beams retrofitted with CFRP and GFRP on the shear capacity of R.C. beams. Results obtained proved that CFRP was better than that of the beams retrofitted with GFRP. D'Souza [13] made U-wraps CFRP with anchors to improve the R.C beam. The results obtained show that the shear strength increased by 120% over the control beam, and the use of anchors provided a large increase in the shear resistance. Al-Rousan and Issa [14] discussed the effect of the a/d ratio on the crack angle, where (a) is the length of the beam and (d) the depth. The results indicated that the beam depth influences the angle. The primary cracking angle varied from 33, 44, 50 and 54 for beams a/d is 2.7, 1.9, 1.5 and 1.2, respectively. The shear crack angle determines how many CFRP strips are intersected by the crack. It also affects whether the intersected strips are fully effective in improving the beam's performance. Feng and Leung [15] examined CFRP strip spacing to improve the degree of shear capacity of R.C beams. The results indicated that the capacity of shear increased gradually with a decrease in CFRP strip spacing. With the increase of the shear span ratio, the moment-curvature relationship of specimens increases linearly in the process of loading. Wang and Fang [16] discussed the effect of the shear span/depth ratio with CFRP strip to improve beam shear capacity. The FRP strips are most effective for large shear span/depth ratios, followed by medium shear span/depth ratios, and are least effective for small shear span/depth ratios. Al-Saawani and El-Sayed and Al-Negheimish [17] studied the effect of shear span/depth ratio on the mode failure of R.C. beams strengthened with CFRP that extended all the way to the supports. The findings indicate that 3.0 was determined to be the essential shear span/depth ratio value. The failure mode of the beams was concrete cover separation (CCS) at this ratio and below, and intermediate crack (IC) debonding for beams with a shear-span/depth ratio greater than 3.0. Abdel-Jaber and Katkhuda [18] investigated how the shear strengthening of R.C. beams was affected by the use of near-surface mounted carbon fiber-reinforced polymer (NSM-CFRP). Concrete with low strength ($f_{cu} = 17$ MPa), medium strength ($f_{cu} = 32$ MPa), and high strength ($f_{cu} = 47$ MPa) is taken into consideration. The ductility of the beams strengthened with NSM-CFRP attached is higher than that of the corresponding control beams, according to experimental load-deflection curves. For all beams reinforced with the identical NSM-CFRP structure, the experimental shear capacity generally rose as the compressive strength increased. Abdo and ahmed [19] studied the shear efficiency of steel R.C beams strengthened with internal stirrups or NSM GFRP reinforcement (or both). The obtained results show that using both stirrups with NSM GFRP leads to an increase of capacity of 142.8–211.7% compared to NSM GFRP R.C beams without internal stirrups. Marwa and Debaiky [20] evaluated various methods for enhancement the shear capacity of R.C. beams by using GFRP strips, bent bars that are positioned close to the surface. When compared to alternative strengthening methods, the results demonstrate that the GFRP strips with side near surface-mounted bent bars improved shear capacity, ductility, and crack propagation more effectively.

Previous studies have made significant contributions to the field of CFRP strengthening for RC beams; however, several limitations persist. Many studies have focused on specific CFRP configurations without fully exploring the impact of varying geometries, such as different slenderness ratios or CFRP coverage percentages across different beam sizes and load conditions. Furthermore, anchorage techniques have often been under-explored, especially their role in preventing debonding and ensuring the long-term effectiveness of CFRP strengthening. Additionally, the economic feasibility of CFRP applications in real-world scenarios has not been adequately addressed in many studies.

The primary aim of this study is to investigate the effectiveness of carbon fiber-reinforced polymer (CFRP) in enhancing the shear capacity of reinforced concrete (RC) beams. This study explores various CFRP configurations, including different lengths of CFRP wrapping, anchorage techniques, and coverage percentages, to provide a comprehensive understanding of how these factors influence the performance of RC beams under shear loads. The innovation of this study lies in its holistic approach, examining not only CFRP's effectiveness in improving shear capacity but also its potential to shift the failure mode from shear to flexural failure, especially in beams with longer shear spans. Additionally, the study introduces the consideration of slenderness ratios and their interaction with CFRP strengthening, a factor that has not been extensively explored in previous research.

This study addresses these limitations by investigating a broader range of CFRP configurations, anchorage techniques, and beam geometries. By considering various slenderness ratios and the impact of different CFRP coverage percentages for each ratio, the study aligns the findings with practical conditions in real-world applications. Furthermore, by incorporating anchorage methods into the analysis, this research provides valuable insights into preventing common issues like early debonding. The findings from this study will contribute to a more comprehensive understanding of CFRP's role in strengthening RC beams, offering practical recommendations that can be applied in engineering practice.

2. Finite element model:

In the present study, a 3D finite element model was used to represent reinforced concrete beams. To reach this goal, the ANSYS V17.0 was used. The library has a 3D solid element that has the capability for crushing and cracking. Also, ANSYS is very suitable for modeling reinforced concrete members. The concrete material is exposed to two possible failure modes, crushing in compression and cracking in tension. To perform this analysis using ANSYS version (17.0), the 3D solid element (SOLID65) was selected as shown in **Fig. 1(a)**, the mechanical characteristics of concrete as shown in **Table 1. (a)**, and concrete stress-strain curve as shown in **Fig. 1(b)**. This material is a high-strength concrete with a compressive strength (f_{cu}) of 40 MPa and a density of 2400 kg/m³. It exhibits a strain (ϵ_y) of 0.003 and a Young's modulus (E) of 27,808 MPa. These properties make it well-suited for structural applications requiring high durability and load-bearing capacity. The material shows significant stiffness and resistance to deformation under stress, making it ideal for use in strengthened beams with CFRP (Carbon Fiber Reinforced Polymer). This combination is particularly useful for evaluating increased capacity and delayed crushing in concrete, enhancing the overall structural performance.

CFRP can be modeled using shell elements like SHELL181 or solid elements if the geometry is complex. The material properties should reflect the anisotropic nature of CFRP. As seen in **Fig.**

1(d), it is a four-node element having six degrees of freedom at each node: rotations about the x, y, and z-axes and translations in the x, y, and z directions., the mechanical characteristics of CFRP are shown in **Table 1. (b)** This material is a high-performance Carbon Fiber Reinforced Polymer (CFRP) with a yield strength (f_y) of 1355 MPa and a Young’s modulus (E) of 115,700 MPa. It has a thickness of 1.3 mm and an elongation at break of 2.15%. These properties indicate that the CFRP offers excellent strength, stiffness, and minimal deformation under stress. It is ideal for structural reinforcement applications, providing high durability and improved load-bearing capacity. The 3D spar element (LINK 180) available in the element library of the (ANSYS) program was used to model the reinforcing steel bars and steel bolts as shown in **Fig. 1(c)**. The mechanical characteristics of transverse steel are shown in **Table 1. (c)**. The mechanical characteristics of steel longitudinal reinforcement are shown in **Table 1. (d)**. The mechanical characteristics of steel bolts used for anchored are shown in **Table 1. (e)**. This material is a high-strength steel with a yield strength (f_y) of 240 MPa and a Young’s modulus (E) of 200,000 MPa. It exhibits a yield strain (ϵ_y) of 0.002, an ultimate strain of 0.008, and a maximum strain of 0.016. These properties demonstrate its excellent ability to withstand stress and deformation, offering high stiffness and strength. The material is suitable for structural applications that require both high load-bearing capacity and significant strain tolerance before failure. Additionally, it can be used for small fixation bolts designed to withstand axial loads.

Table 1. Material characteristics of used materials

(a) Material characteristics of the concrete		(b) Material characteristics of CFRP strips.	
Compressive Strength (f_{cu}) (MPa)	40	Yield strength " f_y " (MPa)	1355
Density(kg/m ³)	2400	Young’s modulus “E” (MPa)	115700
strain “ ϵ_y ”	0.003	Thickness of roll (mm)	1.3
Young’s modulus “E” (MPa)	27808	Elongation at break	2.15%
(c) Material characteristics of the transverse steel		(d) Material characteristics of the steel longitudinal reinforcement	
Yield strength " f_y " (MPa)	240	Yield strength " f_y " (MPa)	360
Young’s modulus “E” (MPa)	200,000	Young’s modulus “E” (MPa)	200,000
Yield strain “ ϵ_y ”	0.002	Yield strain “ ϵ_y ”	0.002
Ultimate strain “ ϵ_y ”	0.008	Ultimate strain “ ϵ_y ”	0.008
maximum strain “ ϵ_y ”	0.016	maximum strain “ ϵ_y ”	0.016
(e) Material characteristics of the anchored steel bolts			
Size “mm”	12		
Tensile resistance Ft,Rd [kN](10.9)	60.7		
Shear resistance per shear plane Fv,Rd [kN]	33.7		

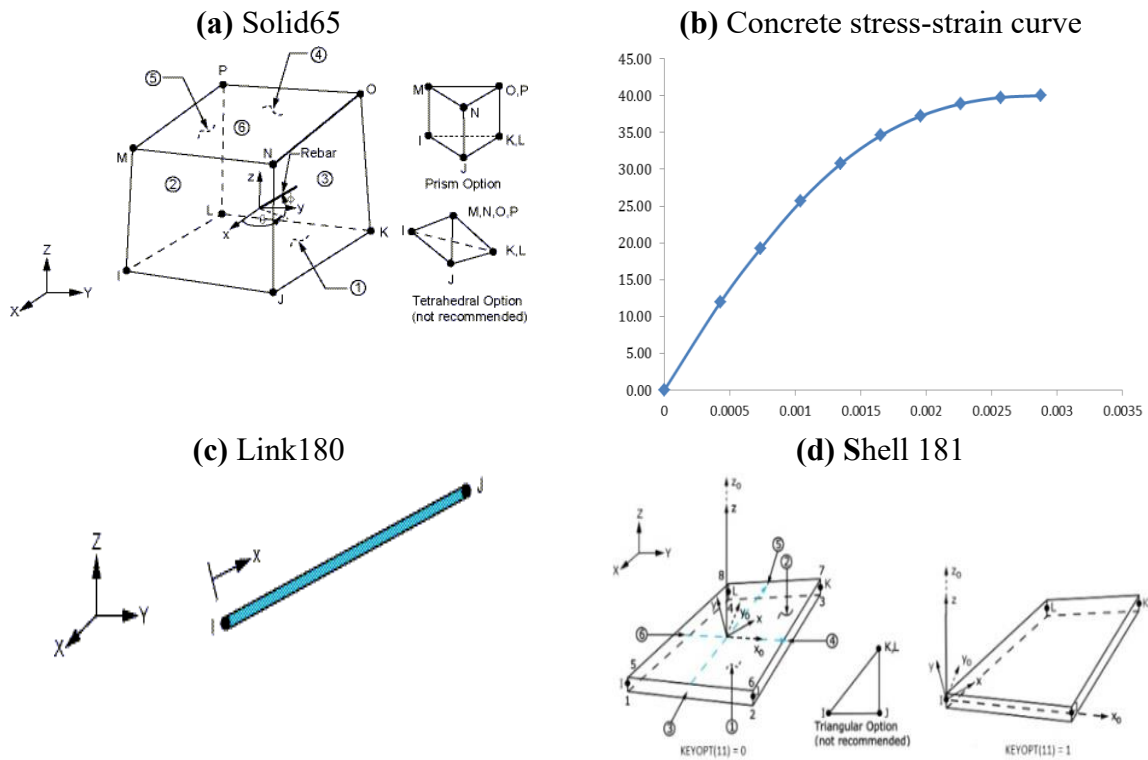


Fig.1. Applied elements (a, c, d), Concrete stress-strain curve (b)

3. Details of RC. beam

The RC. beams with overall dimensions of 120 mm width, 400mm thickness, and variable lengths to thickness ratios were tested, $L= 3T, 4T, 5T$ and $6T$, where L represents the span length of the beam and T refers to total thickness of R.C beam as shown in Fig.2(a).

Beam reinforcement details were high-grade steel, three bars with a diameter of 20 mm and two bars with a diameter of 20 mm as bottom and top reinforcement respectively, In addition, Two branches of normal mild steel bars with a diameter of 8 mm were mounted as transverse steel reinforcement stirrups each 200 mm as shown in Fig.2(b).

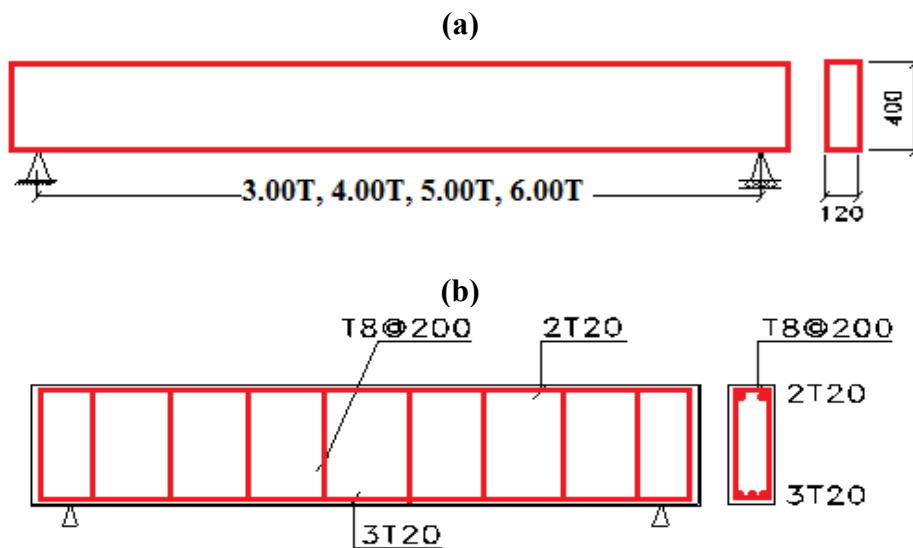


Fig.2. Details of dimensions and reinforcement

4. Verification of the Validity of Finite Element Analysis for Unstrengthened Beam (Control)

ANSYS was utilized to assess the accuracy of the solutions obtained in these studies and to compare the program's results with the experimental data, ensuring the validity and reliability of the modeling process.

4.1. The mechanical characteristics of materials

Mechanical characteristics of materials used in experimental research and their application in finite element analysis. The steel was high tensile steel with yield strength 400 MPa. The mechanical characteristics of high tensile steel as in **Table.2**. The compressive strength of the tested concrete cubes was found to be 40 MPa, as indicated by the stress-strain curve shown in **Figure .3**. The material properties derived from this curve were utilized for the analysis in ANSYS software, as summarized in **Table.3**.

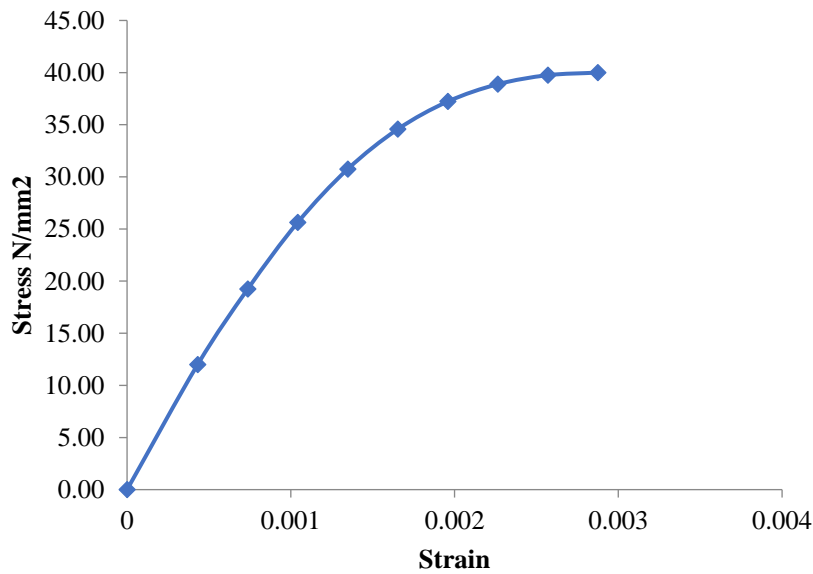


Figure .3. Stress-strain curve

Table.2.Basic mechanical characteristics of high tensile steel

Yield strength “fy” (MPa)	400
Ultimate strength “fu” (MPa)	520
Young’s modulus “E” (MPa)	200,000
Yield strain “εy”	0.002
Ultimate strain “εy”	0.008
maximum strain “εy”	0.016

Table.3. Concrete material properties and coefficients in ANSYS

Constant	Meaning	used
1	Shear transfer coefficients for an open crack	0.5
2	Shear transfer coefficients for a closed crack	0.8
3	Uniaxial tensile cracking stress	4.2
4	Uniaxial crushing stress	40
5	Biaxial crushing stress	0
6	Ambient hydrostatic stress state	0
7	Biaxial crushing stress under the ambient hydrostatic stress state	0
8	Uniaxial crushing stress under the ambient hydrostatic stress state	0
9	Stiffness multiplier for cracked tensile condition	0.6

4.1.3 Details of Experimental Testing and Finite Element Modeling (FEM)

The RC beam with dimensions of 120 mm width, 300mm depth and 2500mm length were tested. The beam was simply supported with a clear span of 2200 mm as shown in **Fig. 4(a)**. The bottom longitudinal reinforcement of specimen was 5 bars with diameter 16 mm, the top longitudinal reinforcement of specimen was 3 bars with diameter 16 mm and 2 bars with diameter 12 mm was located of the top surface distance of 100 mm and were confined in the compression zone with additional vertical stirrups 10 mm bars at 125 mm. The stirrups were 10 mm diameter bars at 125 mm as shown in **Fig. 4(b)**. The test setup for the experimental work demonstrated visible cracking up to failure, as shown in **Fig. 4(c)**. The mesh used in the FEM analysis consisted of 20x20x20 elements, as shown in **Fig. 4(d)**. The modeling process is presented in **Fig. 4(e)**, and the shape of the crack observed during the analysis is illustrated in **Fig. 4(f)**.

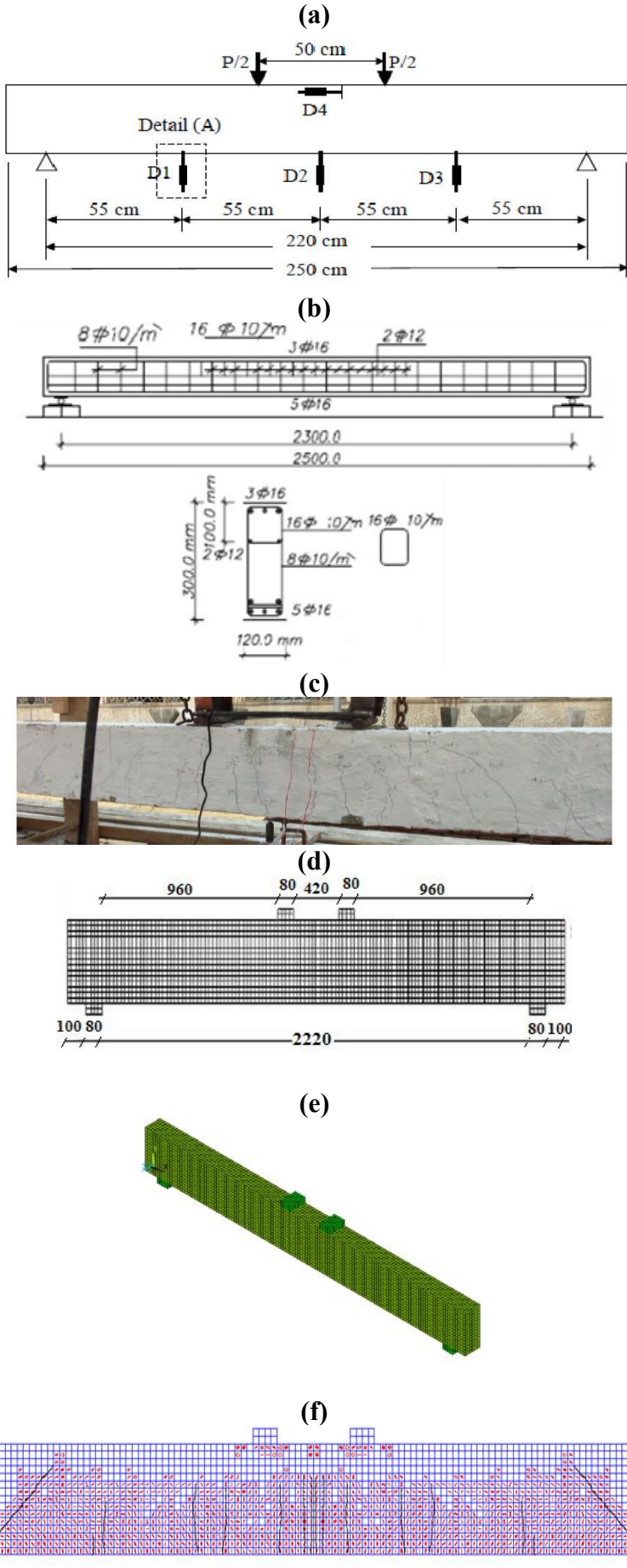


Figure .4. Details of beam analysis and experimental results vs. FEM results

4.1.4 Comparison of results between experimental testing and finite element modeling (FEM)

The comparison aims to assess the agreement and accuracy of material modeling in specific engineering applications. This will contribute to improving the reliability of Finite Element Modeling (FEM) in structural design and analysis. The results as shown in **Table.4**.

Table.4. Comparison of experimental and FEM values

Parameters	EXP	FEA
Pu (kN)	247	239.207
Δu (mm)	-41.96	-34.3365
ε_c max (%)	-0.00755	-0.005921
ε_s max (%)	0.009317	0.0175
Modes of failure	Ductile	Ductile

- **Ultimate Load:** The ultimate load predicted by FEA (239.207 kN) is slightly lower than the experimental value (247 kN), with a difference of about 3.15%. This is a relatively small discrepancy and may be attributed to factors such as simplifications in the FEA model or minor inaccuracies in material properties or boundary conditions used in the analysis.
- **Displacement (Δu):** The displacement calculated by FEA (-34.3365 mm) is smaller than the experimental displacement (-41.96 mm), showing a difference of approximately 18.5%. This suggests that the FEA model may be more sensitive to the initial cracking behavior, capturing deformations earlier in the loading process. In contrast, the experimental results might show visible cracking later due to factors such as the resolution of measurement or human observation limitations in detecting early micro-cracks.
- **Maximum Concrete Strain:** The maximum concrete strain predicted by FEA (-0.005921%) is lower than the experimental value (-0.00755%), with a difference of around 21.6%. This indicates that the FEA model may be underestimating the strain in the concrete, possibly due to a less accurate representation of the concrete's nonlinear behavior in the model.
- **Maximum Steel Strain:** The maximum steel strain from FEA (0.0175%) is noticeably higher than the experimental value (0.009317%). This could suggest that the FEA model is predicting more strain in the steel reinforcement, possibly due to differences in the material properties or stress-strain relationships used for the steel in the simulation. Additionally, it might reflect a difference in the steel yielding behavior in the experimental and FEA conditions.
- **Modes of Failure:** Both the experimental and FEA results indicate ductile failure, which is consistent and suggests that the FEA model is capturing the general failure mechanism of the specimen correctly. However, the exact nature of the failure, such as the local failure points or cracking patterns, might differ slightly between the two due to model simplifications in the FEA.

4.2 Verification of the Validity of Finite Element Analysis for strengthened Beam with steel angel

The comparison aims to assess the agreement and accuracy of material modeling in specific engineering applications. This will contribute to enhancing the reliability of Finite Element

Modeling (FEM) in structural design and analysis, particularly for beams strengthened with steel angles to ensure flexural failure. The results are presented in **Table .5**. The mode of failure is shown in **Figure .5**, for both experimental and FEM results.

Table.5. Comparison (EXP), (FEA)

Parameters	EXP	ANSYS
P_u (KN)	130	117
Δ_u (mm)	7.25	6.23
Modes of failure	Shear	Shear

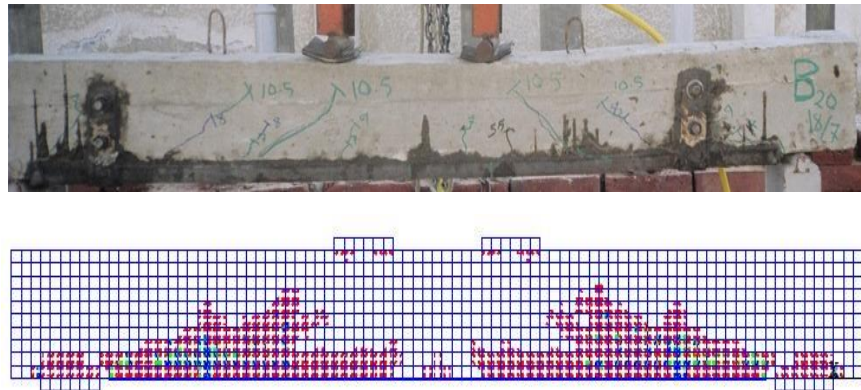


Fig. 5. Details of beam analysis and experimental results vs. FEM results

Ultimate Load(P_u): The ultimate load predicted by ANSYS (117 kN) is slightly lower than the experimental value (130 kN), with a difference of about 10%. This discrepancy may be due to differences in material properties, boundary conditions, or model simplifications in the ANSYS simulation. While this difference is not very large, it highlights the importance of accurately defining material models and loading conditions in FEM simulations.

Displacement (Δ_u): The displacement calculated by ANSYS (6.23 mm) is smaller than the experimental value (7.25 mm), showing a difference of approximately 14%. This could be due to the stiffness of the model being higher in the simulation, possibly because of idealized boundary conditions or the linear material model used in ANSYS compared to the real behavior in the experiment, in addition the FEA model may be more sensitive to the initial cracking behavior, capturing deformations earlier in the loading process. In contrast, the experimental results might show visible cracking later due to factors such as the resolution of measurement or human observation limitations in detecting early micro-cracks.

Modes of Failure: Both experimental testing and ANSYS simulations predict shear failure, indicating that the FEA model accurately captures the failure mode under the given conditions.

4.3 Verification of the Validity of Finite Element Analysis for strengthened Beam with CFRP strips

The performance of these strengthened structures must be verified against experimental results. This study aims to verify the validity of FEA simulations for beams strengthened with CFRP strips, focusing on parameters such as load-bearing capacity, displacement, and failure modes. By comparing the results from both experimental tests and FEA, this research seeks to assess the reliability of FEA models in predicting the enhanced performance of CFRP-strengthened beams and their failure mechanisms. RC beam details was shown in **Fig.6**.

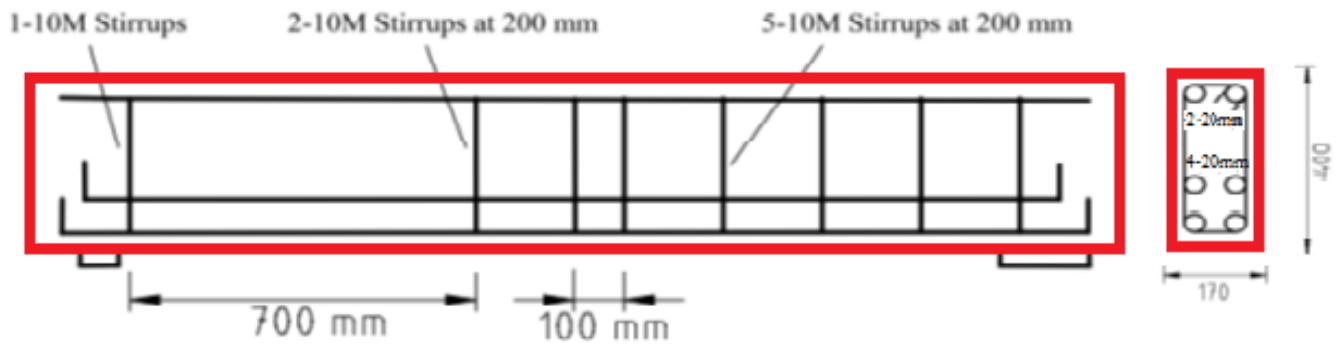


Fig. 6. Details of concrete dimensions and reinforcement details in the beam

4.3.1 The mechanical characteristics of materials

Mechanical Characteristics of Materials Used in Experimental Research and Their Application in Finite Element Analysis.

4.3.2 Compressive strength of the tested cubes

The compressive strength of the tested concrete cubes was found to be 40 MPa, as indicated by the stress-strain curve shown in **Figure .7**. The material properties derived from this curve were utilized for the analysis in ANSYS software, as summarized in **Table.6**.

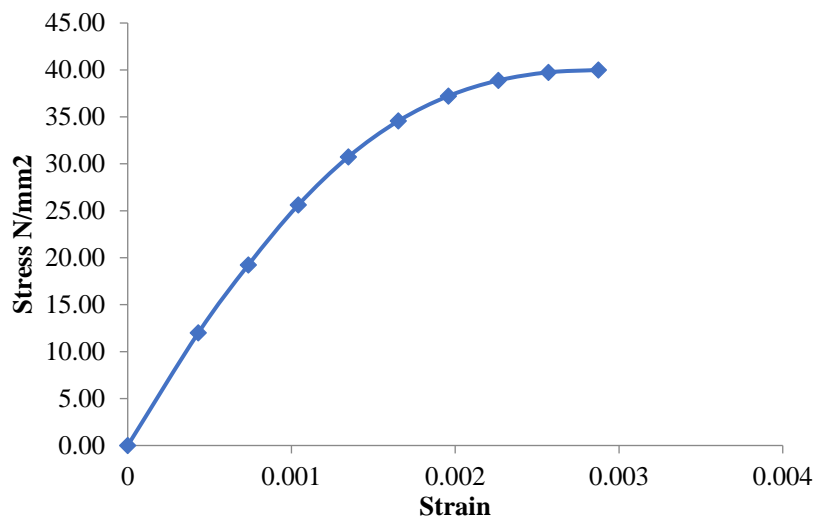


Figure .7. Stress-strain curve

Table.6. Concrete material properties and coefficients in ANSYS

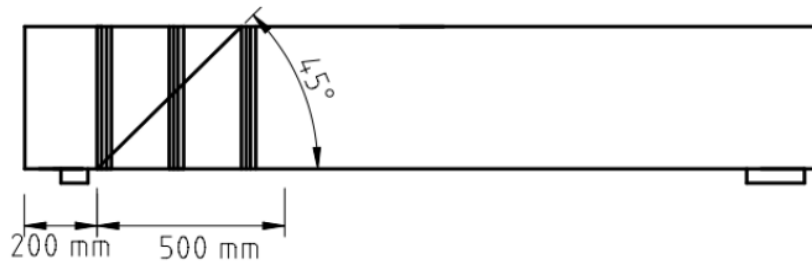
Constant	Meaning	used
1	Shear transfer coefficients for an open crack	0.5
2	Shear transfer coefficients for a closed crack	0.8
3	Uniaxial tensile cracking stress	4.2
4	Uniaxial crushing stress	40
5	Biaxial crushing stress	0
6	Ambient hydrostatic stress state	0
7	Biaxial crushing stress under the ambient hydrostatic stress state	0
8	Uniaxial crushing stress under the ambient hydrostatic stress state	0
9	Stiffness multiplier for cracked tensile condition	0.6

4.3.3 Steel reinforcement

Grade 400 steel was used for the longitudinal tensile and compressive reinforcement, as well as for the internal shear reinforcement. The tensile and compressive longitudinal reinforcement consisted of 20M bars. Tensile tests in accordance with the ASTM A370 (2016) guidelines were performed on three 500 mm length steel specimens from the same batch as the steel used for the longitudinal reinforcement in the beams.

4.3.4 Carbon-fiber Sheet

The SikaWrap 1400C carbon-fibre fabric was used in this experimental study to produce the U-wraps, full wraps, and anchor head plates used to strengthen the test specimens. The SikaWrap 1400C is a unidirectional, high strength carbon fibre fabric that is flexible and can be wrapped around complex geometries. FRP is an elastic material up to failure, therefore the stress in the FRP can be determined at any value of strain using its modulus of elasticity. The physical and mechanical properties of the SikaWrap 1400C carbon-fibre sheet as reported by the manufacturer, as shown in **Table .7**. Sika Canada Inc ® (<https://can.sika.com/>), set up of wrapping as shown in **Figure .8**.

**Figure .8.** Arrangement of the wrapping setup**Table .7.** Mechanical Properties of Sika Wrap 1400C

Property	Value
Tensile Strength	1355 Mpa
Modulus of Elasticity	115700 Mpa
Elongation at Break	2.15%
Thickness	1.3 mm
Colour	Black

4.3.5 Comparison of results between experimental testing and finite element modeling (FEM)

The comparison aims to assess the shear capacity results obtained from experimental testing and FEM simulations to evaluate the accuracy of FEM in predicting the behavior of CFRP-strengthened beams. By examining key parameters such as shear strength, displacement, and failure modes, this research seeks to validate the reliability of FEM for the design and analysis of CFRP-strengthened RC beams. As shown in **Table.5**.

Table.8. Show the comparison between FEM and EXP

Parameters	EXP	FEA
P_u (KN)	346	350
Δ_u (mm)	43.2	29.3
Modes of failure	Flexure (compression zone)	Flexure (compression zone)

The overall agreement between experimental results and FEA predictions is fairly good, particularly regarding the ultimate load and failure mode. However, the significant difference in displacement suggests that the FEA model may be more sensitive to the initial cracking behavior, capturing deformations earlier in the loading process. In contrast, the experimental results may show visible cracking later due to factors such as measurement resolution or human limitations in detecting early micro-cracks. The cracks at failure in the experiment are shown in **Figure .9a**, while the cracks at failure in ANSYS are presented in **Figure .9b**. The mode of failure in ANSYS is illustrated in **Figure 9c**, showing the stress at the failure load

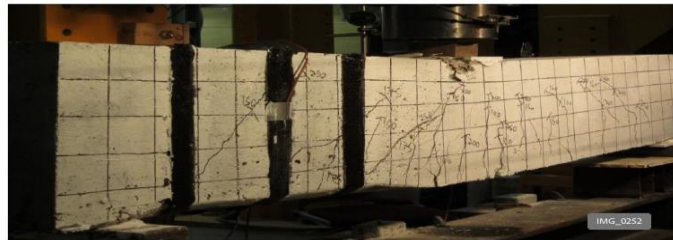


Figure (9a)

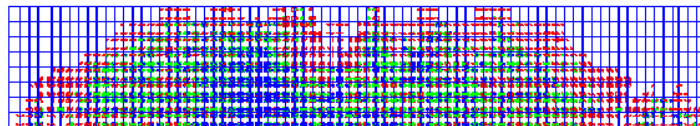


Figure (9b)

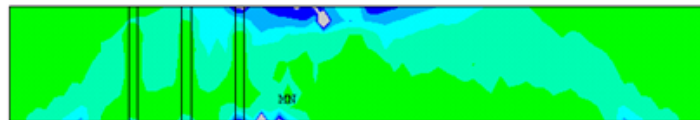


Figure (9c)

Figure .9. Details of beam analysis and experimental results vs. FEM results

5. Numerical paramtric study

A parametric study was conducted to investigate the effectiveness of using CFRP with four different percentages (12.5%, 25%, 37.5%, and 50%) relative to the effective shear zone area, as shown in **Figure .10a**. The CFRP was wrapped around the beam in a U-shape with anchors to strengthen the reinforced concrete (R.C.) beams against shear failure, as illustrated in **Figure .10b**. All the studied cases are summarized in Table 6. The load location is shown in **Fig. 10c**, and the details of the simulation models are presented in **Fig. 10d**



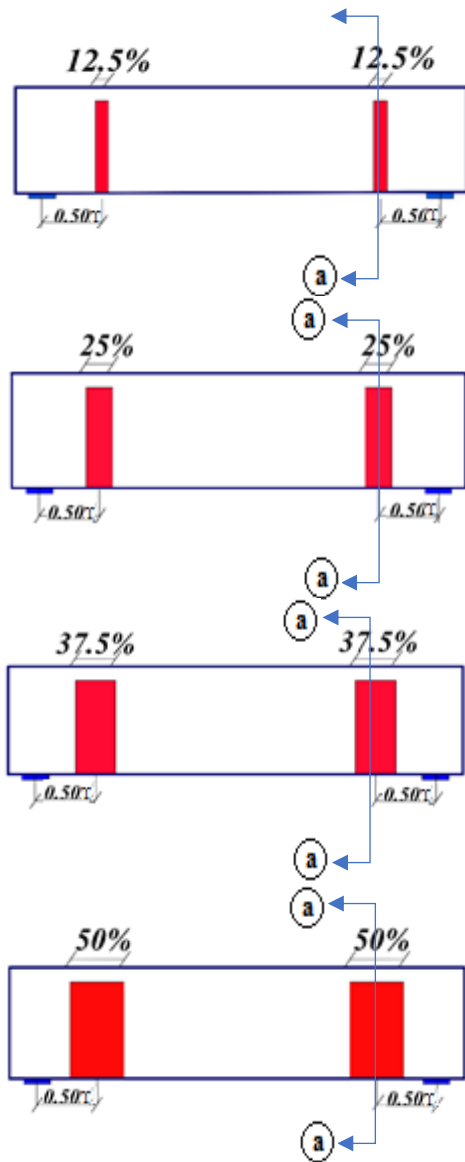


Fig. 10a. Different percentages of CFRI strengthen coverage

Table. 9. RC. beams parameters

Span	Details of strengthen coverage		
	Position of center group	Strengthen coverage area %	Thickness
3 T	0.50 T	12.5	1.30 mm
		25	
		37.5	
		50	
4 T		12.5	
		25	
		37.5	
		50	
5 T		12.5	
		25	
		37.5	
		50	
6 T	12.5		
	25		
	37.5		
	50		

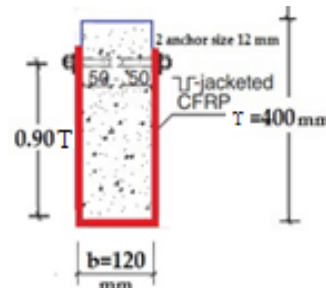


Fig. 10b. Details of sec(a-a)-Typical anchored

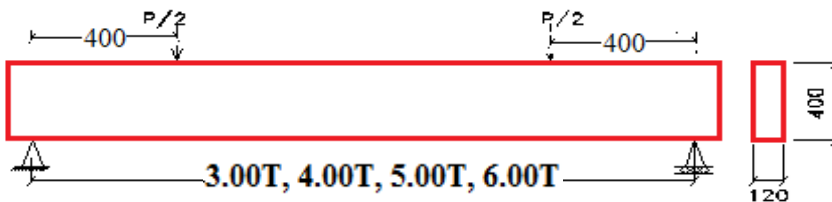


Fig. 10c. Details of the studied beam

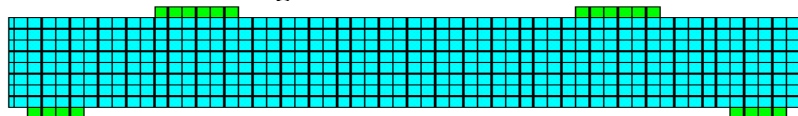


Fig. 10d. 3D simulation model of beam

6. Numerical results

From the parametric study, we represent and analyze these parameters, (a) finite element model strengthen coverage, (b) vertical deformation to identify regions of maximum deformation, (c) von

Mises stress to predict potential failure regions and compare the stress distribution across different configurations, **(d)** stress in the stirrups to evaluate their performance under shear loading. The results observed that the deformation was increased as the length-to-thickness ratio (L/T) of the beams increased, an increase in the cover ratio was associated with enhanced beam capacity. In addition, it was noted that the internal shear reinforcement exceeded the maximum design limits.

The obtained results were divided into the following categories according to length-to-thickness ratio as follows:

6.1. Length to depth equal 3 ($L/T=3$)

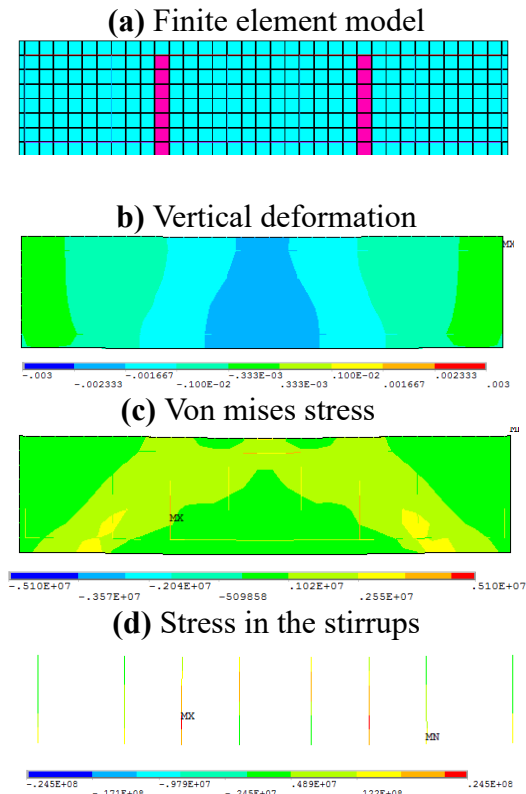


Fig. 11. Finite element model strengthening coverage (12.5%).

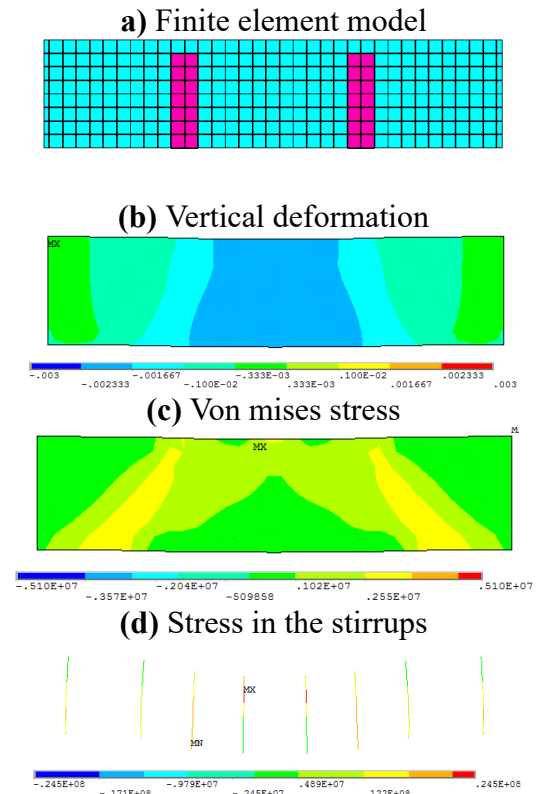


Fig. 12. Finite element model strengthening coverage (25%).

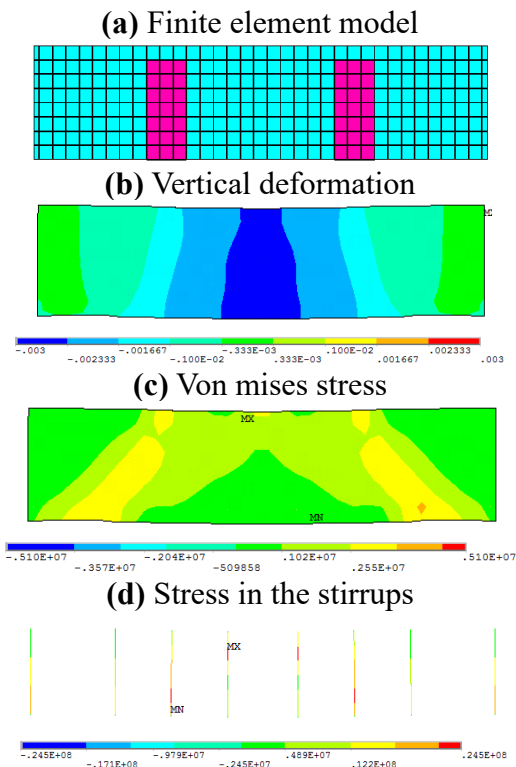


Fig. 13. Finite element model strengthening coverage (37.5%).

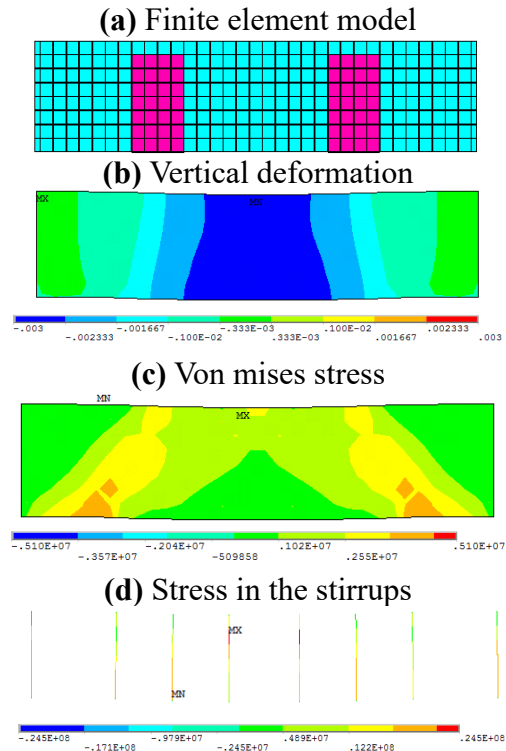


Fig. 14. Finite element model strengthening coverage (50%).

6.2. Length to depth equal 4 (L/T=4)

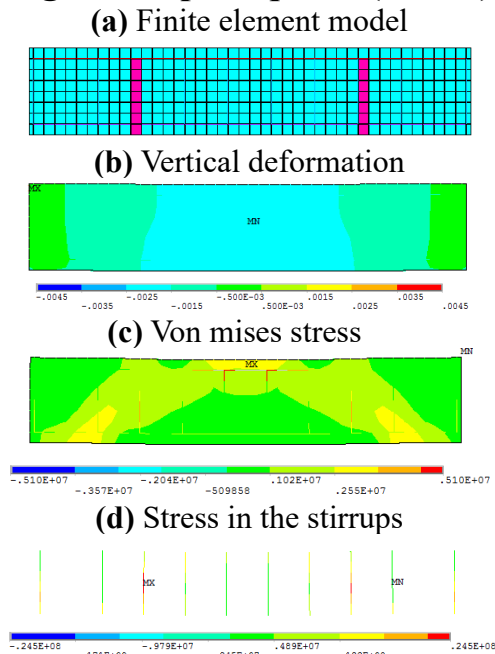


Fig. 15. Finite element model strengthening coverage (12.5%).

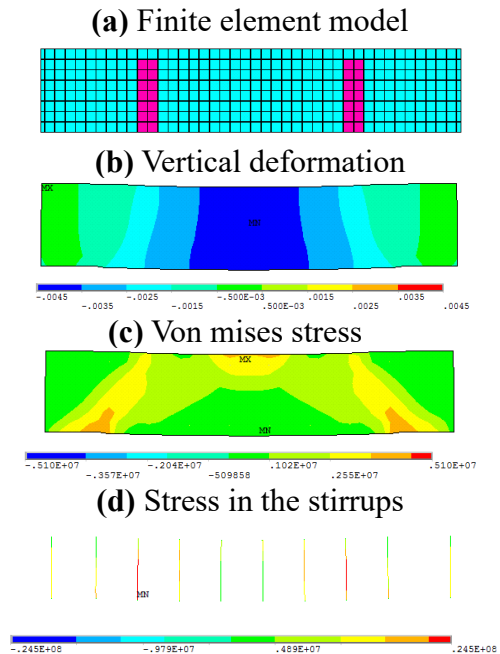


Fig. 16. Finite element model strengthening coverage (25%).

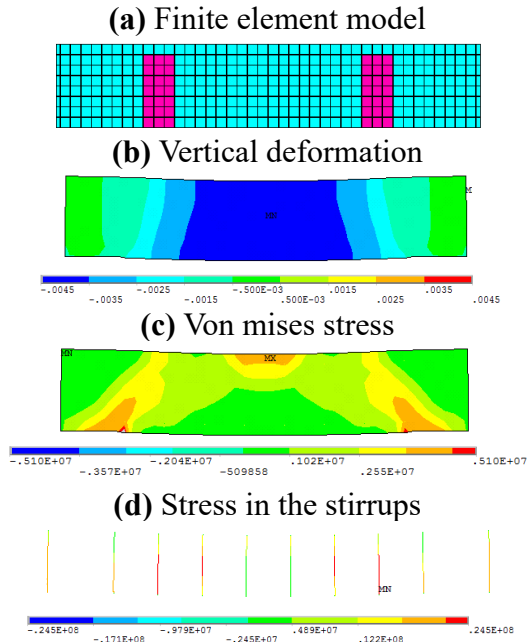


Fig. 17. Finite element model strengthening coverage (37.5%).

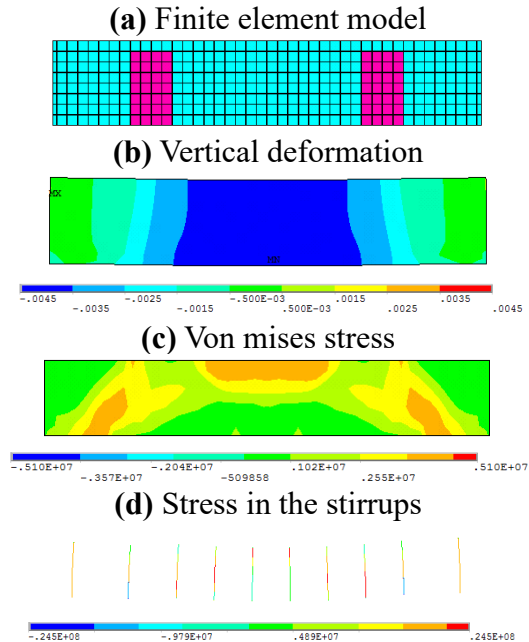


Fig. 18. Finite element model strengthening coverage (50%).

6.3. Length to depth equal 5 ($L/T=5$)

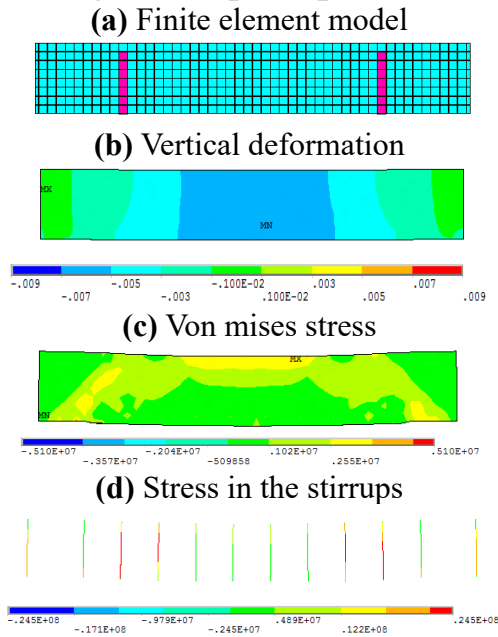


Fig. 19. Finite element model strengthening coverage (12.5%).

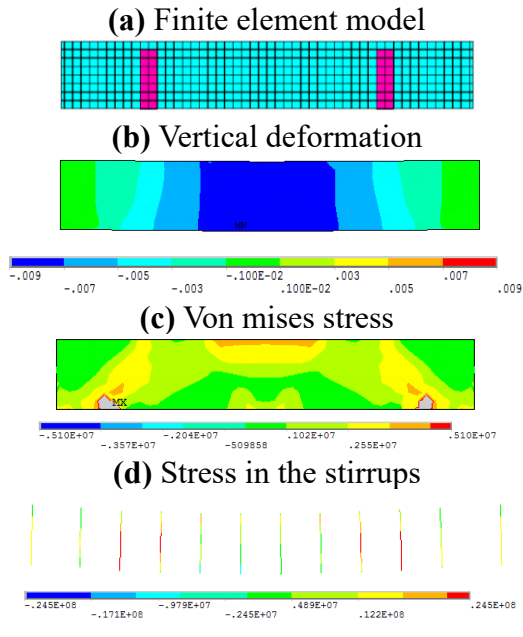


Fig. 20. Finite element model strengthening coverage (25%).

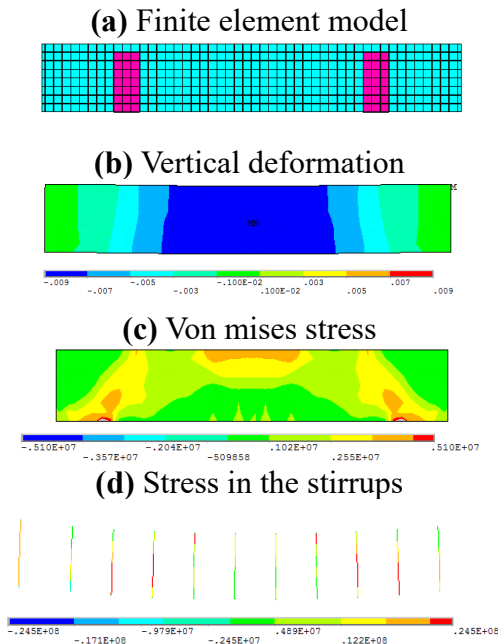


Fig. 21. Finite element model strengthening coverage (37.5%).

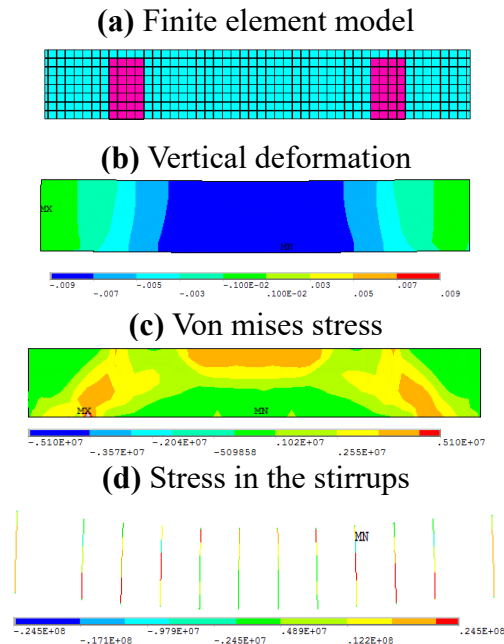


Fig. 22. Finite element model strengthening coverage (50%).

6.4. Length to depth equal 6 (L/T=6)

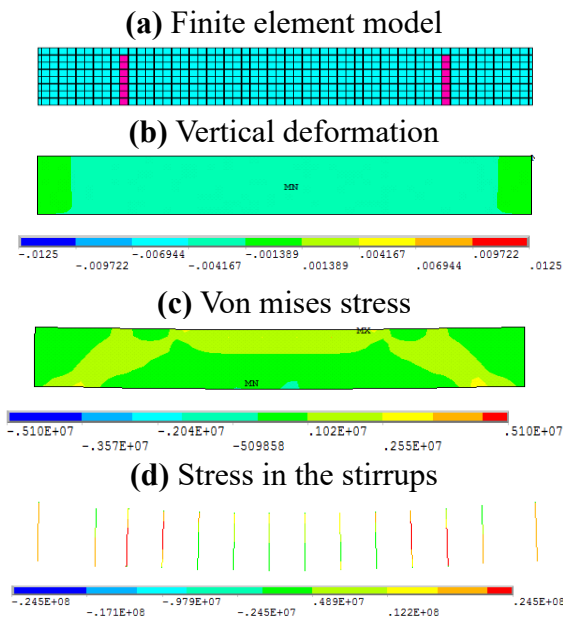


Fig. 23. Finite element model strengthening coverage (12.5%).

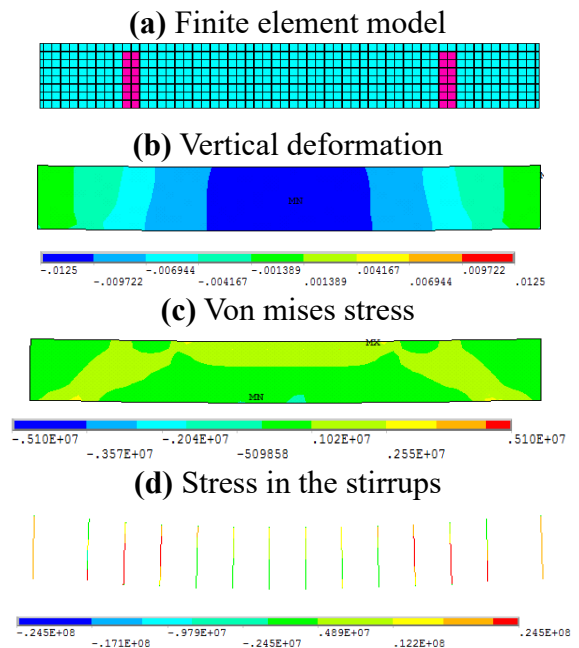


Fig. 24. Finite element model strengthening coverage (25%).

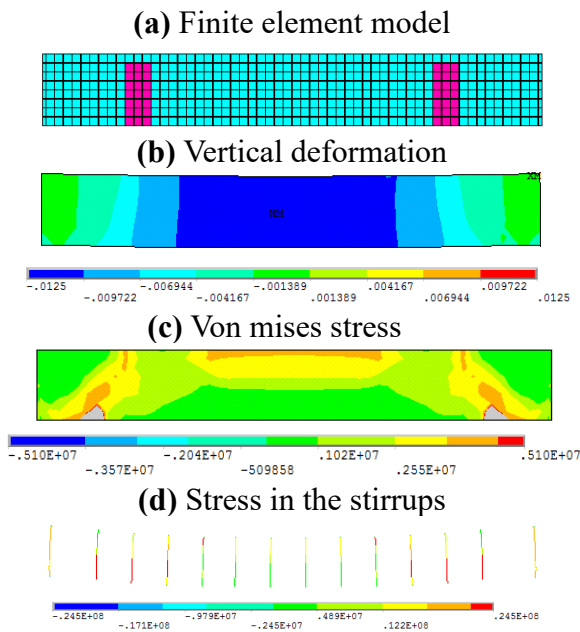


Fig. 25. Finite element model strengthening coverage (37.5%).

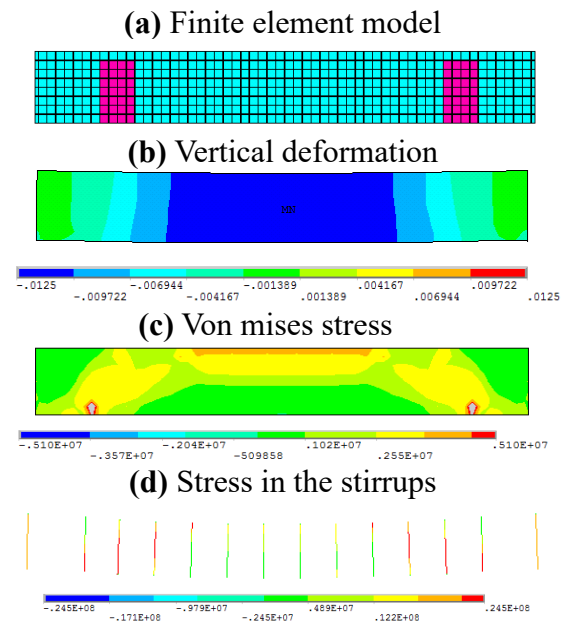


Fig. 26. Finite element model strengthening coverage (50%).

7. Stresses in CFRP material used in strengthening RC beams

The evaluation of stresses is crucial for optimizing the application of CFRP in construction and ensuring long-term reliability. The Fig.22. Below illustrates the Von Mises stress distribution, which helps assess the effectiveness of different percentages of CFRP coverage across varying length-to-thickness (L/T) ratios.

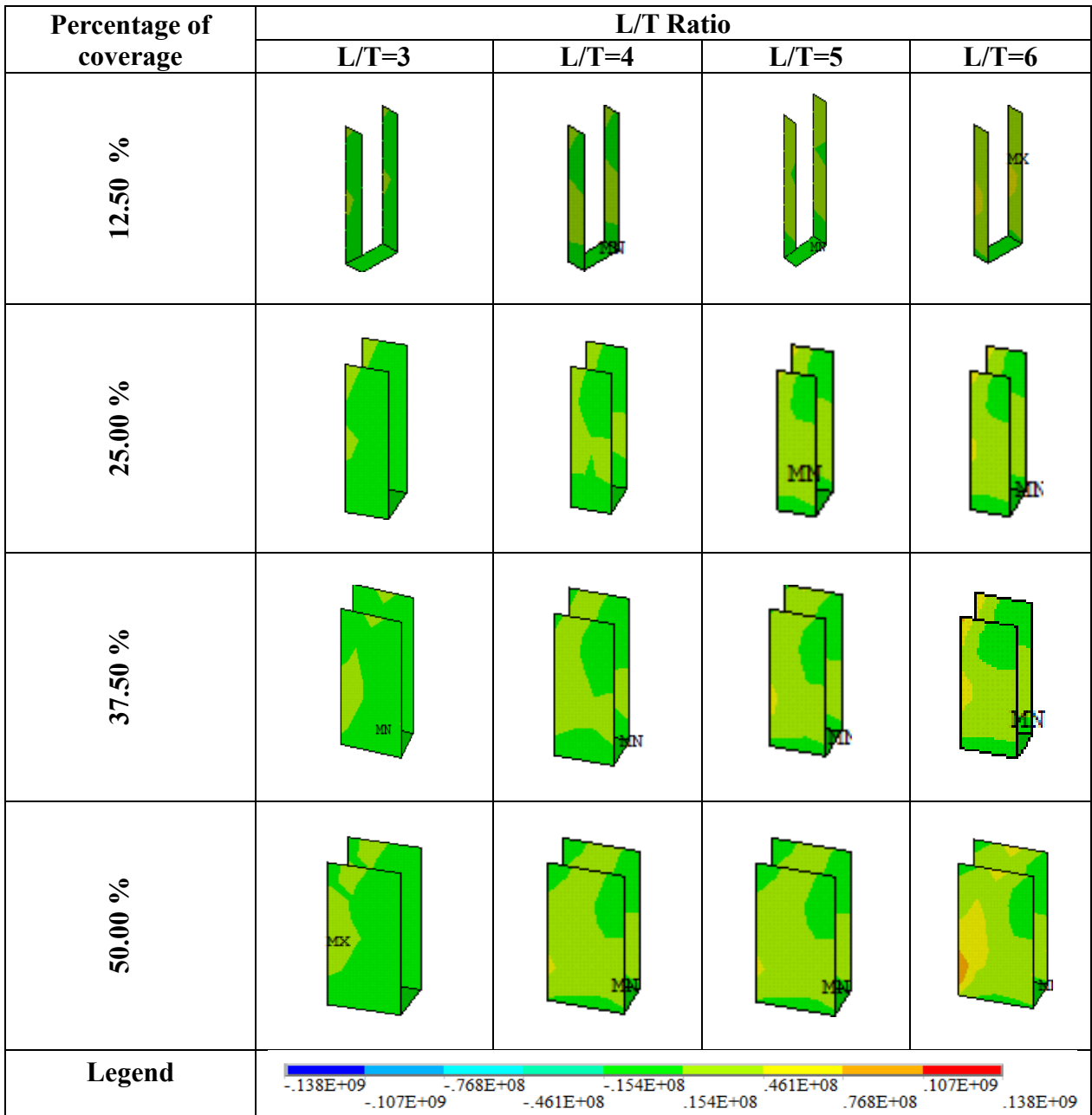


Fig.27 Stress distribution on CFRP

Effect of percentage coverage: Increasing the coverage percentage reduces the stress concentration in the CFRP material. At 12.5% coverage, the stress concentration appears to be localized, indicating limited effectiveness. As the coverage percentage increases to 50%, the stress is more evenly distributed, showcasing enhanced load-bearing capability.

Effect of L/T Ratio: For lower L/T ratios, the stress distribution appears relatively consistent across the coverage levels, suggesting minimal influence of geometry at these dimensions. For higher L/T ratios, stress becomes more localized at lower coverage levels, highlighting the critical need for higher coverage to reduce stress concentration.

Overall, the results confirm the importance of optimizing coverage and geometry for effective use of CFRP in structural applications.

8. Analysis of results

Analysis of the obtained results has been conducted to evaluate the efficiency of using CFRP to enhance shear capacity. The shape of wrapping around the beam was in a U-shape with anchors, and four different percentages 12.5%, 25%, 37.5% and 50% related to effective shear zone area have been studied, in addition, four different length-to-depth ratios, 3, 4, 5 and 6 have been considered in the analysis.

8.1. Effect of L/T ratio on beam shear capacity

Length to depth ratio (L/T) is an indicator of the slenderness ratio of a beam, where L represents the span length of the beam and T is the total thickness of RC. beam.

8.1.1 Effect of (L/T) ratio on Load-Deflection

Figures (22) to (25) show the relation between load(kN) and deflections for L/T equal 3,4,5 and 6, four different ratios of covered area 12.5%, 25%, 37.5% and 50%. Increasing the covered area of the CFRP wrapping leads to improved ductility of the beams and increased deflection.

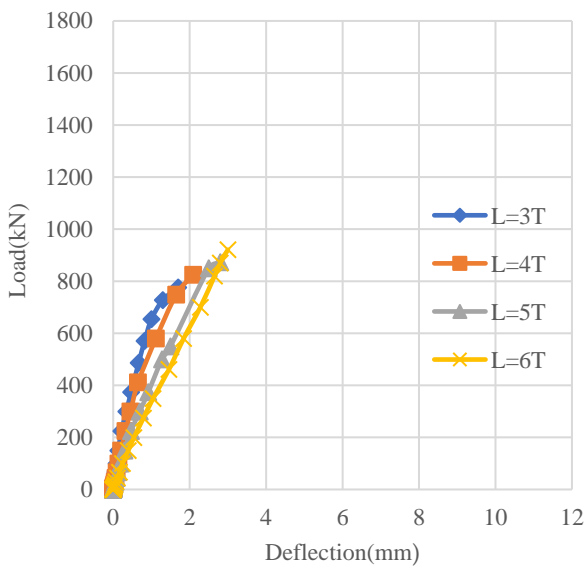


Fig. 28. Load-deflection of U- anchored wrapped-Strengthen coverage (12.5%)

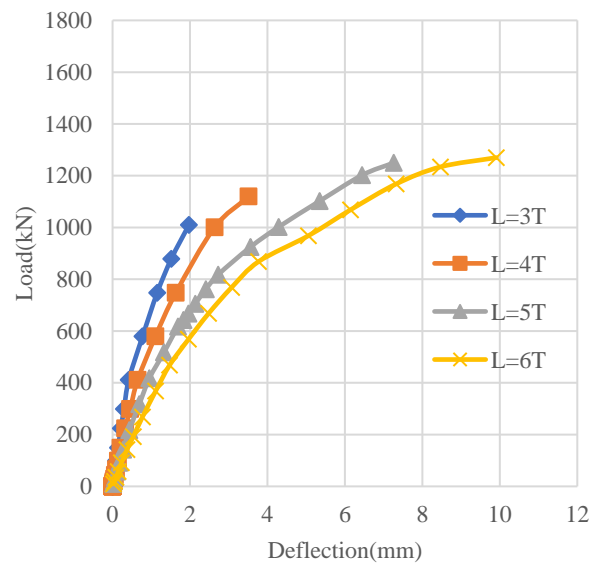


Fig. 29. Load-deflection of U- anchored wrapped-Strengthen coverage (25%)

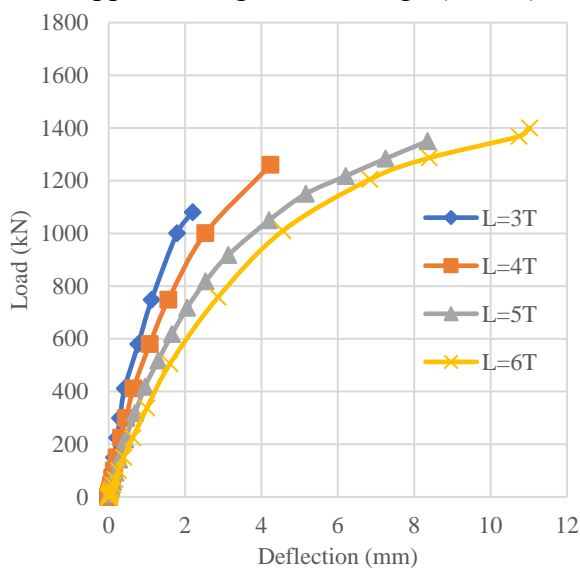


Fig. 30. Load-deflection of U- anchored wrapped-Strengthen coverage (37.5%)

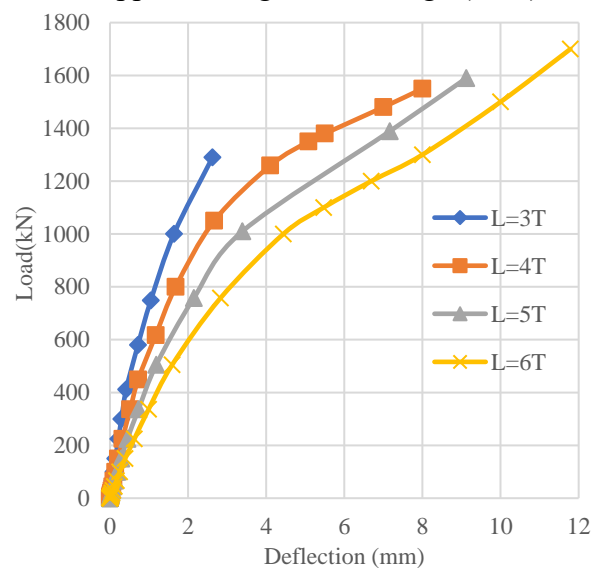


Fig. 31. Load-deflection of U- anchored wrapped-Strengthen coverage (50%)

8.1.2 Effect of L/T ratios on beam shear capacity

Figures (26) to (29) show the relation between load (kN) and covered area 12.5%, 25%, 37.5% and 50%. Increasing the slenderness ratio (L/T) significantly enhances shear capacity from 21.2% to 150%.

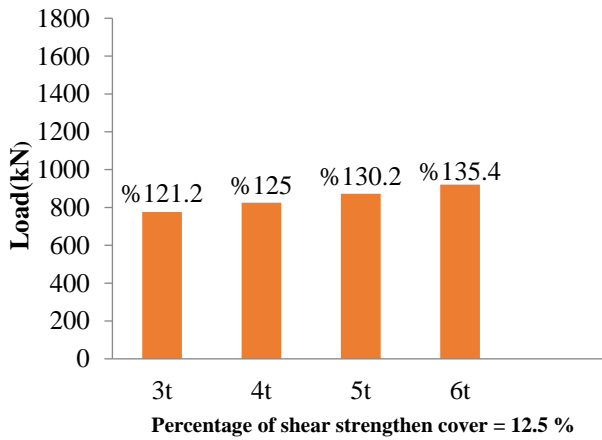


Fig. 32. Load-span for strenghen coverage 12.5%

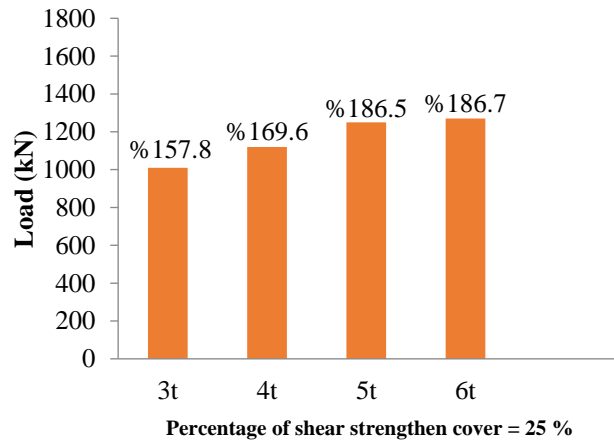


Fig. 33. Load-span for strenghen coverage 25%

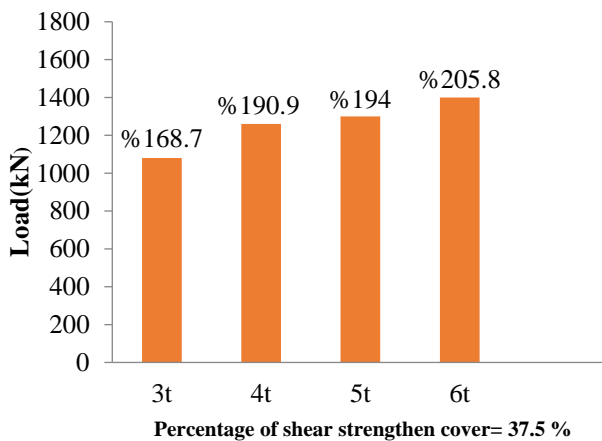


Fig. 34. Load-span for strenghen coverage 37.5%

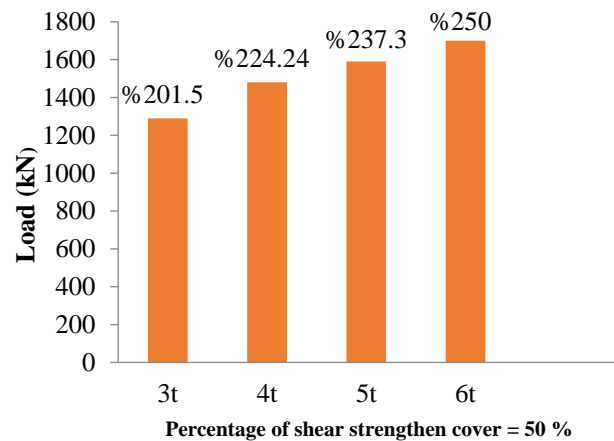


Fig. 35. Load-span for strenghen coverage 50%

9. Effect of strengthening coverage area on beam shear capacity

The effect of different CFRP covering percentages (12.5%, 25%, 37.5%, and 50%) on the shear capacity of beams was analyzed by evaluating the relationship between load and deflection for varying L/T ratios (3, 4, 5, and 6). The study also investigated how each covering percentage influenced the shear capacity for each L/T ratio.

9.1 Effect of cover area on Load-Deflection

Figures (30) to (33) show the relation between load(kN) and deflections(mm) for the covered area 12.5%, 25%, 37.5% and 50% and control beam. Different L/T ratios 3,4,5 and 6 are considered in the following figures. The result showed that increasing CFRP coverage from 12.5% to 50% for beams with an L/T ratio of 3 to 6 leads to an improvement in shear capacity, ranging from 21.2% to 150%.

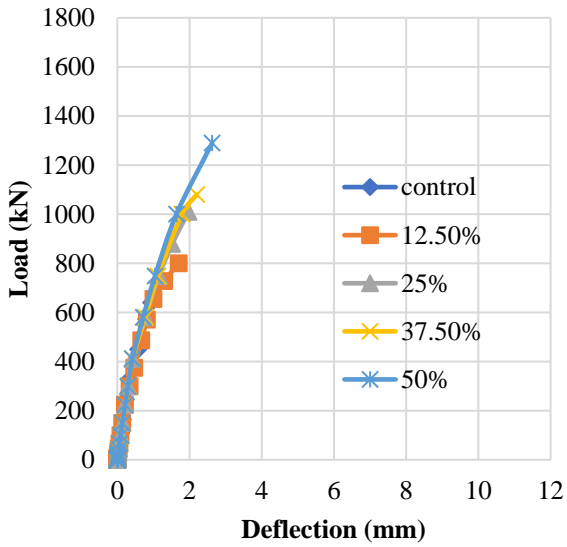


Fig. 36. Load-deflection of RC beam with $L/T=3$ wrapped with anchored U-shape

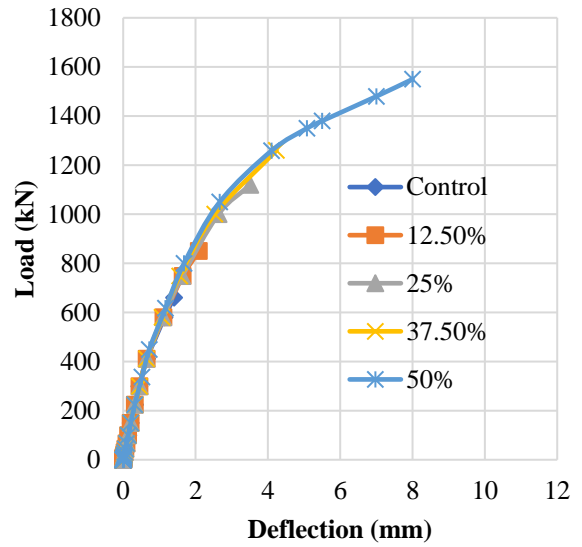


Fig. 37. Load-deflection of RC beam with $L/T=4$ wrapped with anchored U-shape

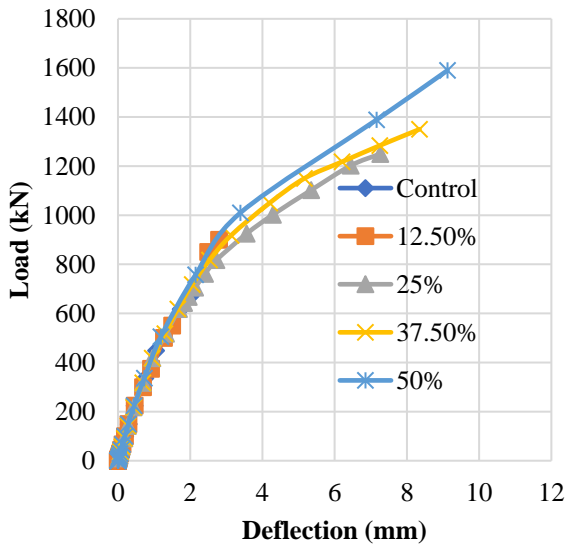


Fig. 38. Load-deflection of RC beam with $L/T=5$ wrapped with anchored U-shape

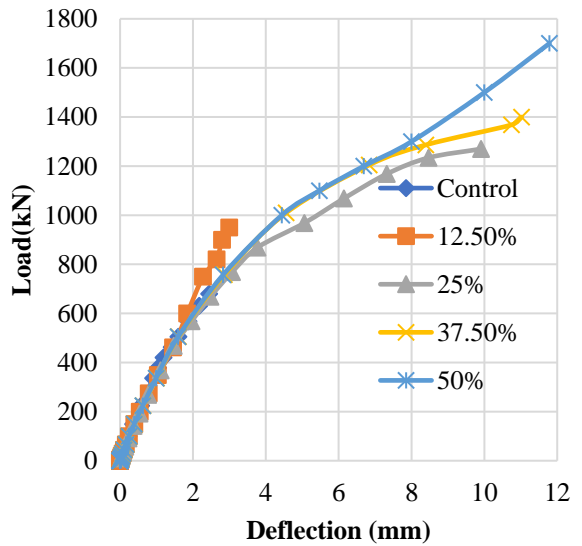


Fig. 39. Load-deflection of RC beam with $L/T=6$ wrapped with anchored U-shape

9.2. Effect of covered area on beam shear capacity.

Figures (34) to (37) show the relation between load(kN) and percentage of the covered area starting from zero (control beam) to 50% related to effective shear zone area, different L/t ratios are studied. Increasing the percentage of the covered area from 12.5% to 50% significantly enhances shear capacity from 21.2% to 150% related to the control beam.

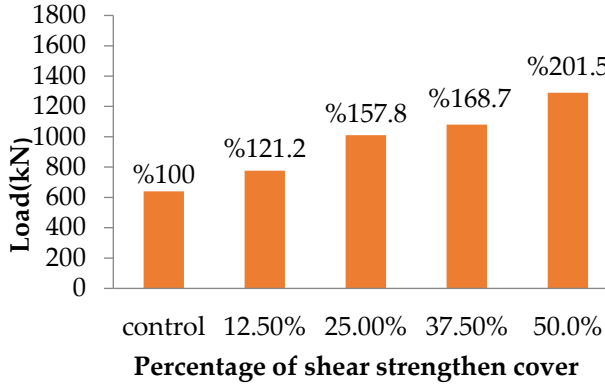


Fig. 40. Length to depth equal 3 (L=3 T)

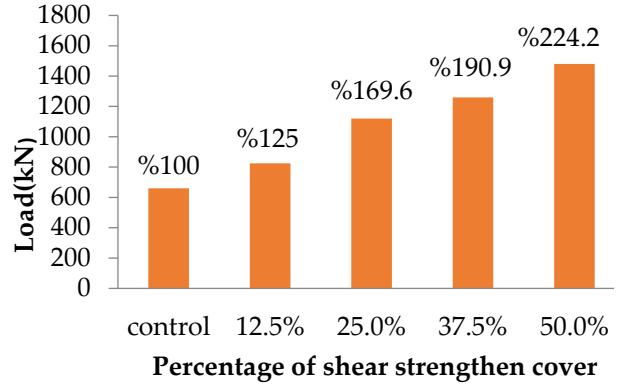


Fig. 41. Length to depth equal 4 (L=4 T)

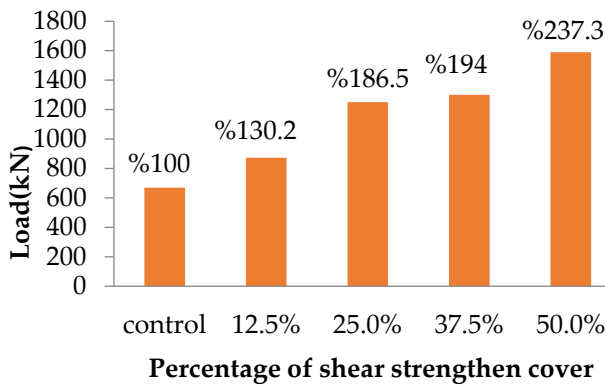


Fig. 42. Length to depth equal 5 (L=5 T)

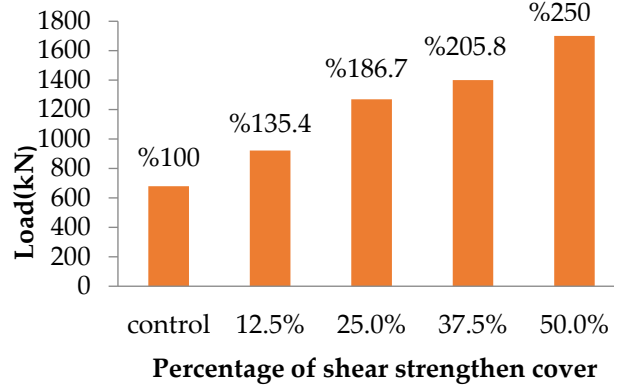


Fig. 43. Length to depth equal 6 (L=6 T)

Conclusions

- The use of CFRP strengthening can shift the failure mode from shear to flexure, particularly in beams with longer shear spans.
- CFRP wrapped around the beam in a U-shape with anchor bolts significantly improves the shear capacity of the beam.
- CFRP improved the ductility of the RC beam, leading to greater enhancements in shear capacity.
- The use of CFRP significantly contributes to enabling the shear reinforcement (Stirrups) to achieve their maximum yield stress.
- Using CFRP coverage from 12.5% to 50% for beams with an L/T ratio of 3 to 6 leads to an improvement in shear capacity, ranging from 21.2% to 150%.

References

- [1] Abeel-Halim, M. A., & Schorn, H. (1989). Strength evaluation of shotcrete-repaired beams. *Structural Journal*, Vol.86, No.3, PP.272-276.
- [2] Chajes, M. J., Thomson Jr, T. A., Januszka, T. F., & Finch Jr, W. W. (1994). Flexural strengthening of concrete beams using externally bonded composite materials. *Construction and Building Materials*, Vol.8, No.3, PP. 191-201.
- [3] Garden, H. N., Quantrill, R. J., Hollaway, L. C., Thorne, A. M., & Parke, G. A. R. (1998). An experimental study of the anchorage length of carbon fibre composite plates used to strengthen reinforced concrete beams. *Construction and Building Materials*, Vol.12, No.4, PP. 203-219.
- [4] Abdel-Jaber, M. S., Walker, P. R., & Hutchinson, A. R. (2003). Shear strengthening of reinforced concrete beams using different configurations of externally bonded carbon fibre reinforced plates. *Materials and Structures*, Vol.36, PP .291-301.
- [5] Zhang, Z., Hsu, C. T. T., & Moren, J. (2004). Shear strengthening of reinforced concrete deep beams using carbon fiber reinforced polymer laminates. *Journal of Composites for Construction*, Vol.8, No.5, PP .403-414.
- [6] El Thakeb, A., Asran, A., El Sebai, A., El Esnawi, H. and Amer, A. (2005), "Enhancement Of Serviceability And Flexural Properties Of Strengthened And Rehabilitated Reinforced Concrete Beams" , *Al-Azhar University Engineering Journal*, AUEJ, Vol. 8, No. 10, PP. 52-67
- [7] Tanarlan, H. M., Ertutar, Y., & Altin, S. (2008). The effects of CFRP strips for improving shear capacity of RC beams. *Journal of Reinforced Plastics and Composites*, Vol. 27, No. 12, PP 1287-1308.
- [8] Ibrahim, A. M., & Mahmood, M. S. (2009). Finite element modeling of reinforced concrete beams strengthened with FRP laminates. *European Journal of Scientific Research*, Vol.30, No.4, PP526-541.
- [9] Tanarlan, H. M. (2011). The effects of NSM CFRP reinforcements for improving the shear capacity of RC beams. *Construction and Building Materials*, Vol. 25, No. 5, PP.2663-2673.
- [10] A. Vijayakumar, Dr.D.L.Venkatesh babu and R. Jayaprakash.(2012). Analytical study on various types of FRP beams by using ANSYS, *International Journal of Engineering Research and Applications*, Vol.2, PP.593-98.
- [11] Jayajothi, p., kumutha, r., & vijai, k. (2013). Finite element analysis of frp strengthened rc beams using ansys, Vol.14, No.4, PP.631-642.
- [12] Jayalin.D , Prince arulraj. g , karthika.v. (2015). analysis of composite beam using ansys. *international journal of research in engineering and technology*
- [13] D'Souza, C. (2016). Shear strengthening of RC beams using externally bonded and anchored FRP U-wraps (Doctoral dissertation).
- [14] Al-Rousan, R. Z., & Issa, M. A. (2016). The effect of beam depth on the shear behavior of reinforced concrete beams externally strengthened with carbon fiber-reinforced polymer composites. *Advances in Structural Engineering*, Vol.19, No. 11, PP.1769-1779.
- [15] Li, W., & Leung, C. K. (2016). Shear span-depth ratio effect on behavior of RC beam shear strengthened with full-wrapping FRP strip. *Journal of Composites for Construction*, Vol.20, No.3, PP.04015067.
- [16] Yu, F., Guo, S., Wang, S., & Fang, Y. (2019). Experimental study on high pre-cracked RC beams shear-strengthened with CFRP strips. *Composite Structures*, Vol. 225, PP.111163.

- [17] Al-Saawani, M. A., El-Sayed, A. K., & Al-Negheimish, A. I. (2020). Effect of shear-span/depth ratio on debonding failures of FRP-strengthened RC beams. *Journal of Building Engineering*, Vol.32, PP.101771.
- [18] Abdel-Jaber, M. E., Abdel-Jaber, M. T., Katkhuda, H., Shatarat, N., & El-Nimri, R. (2021). Influence of compressive strength of concrete on shear strengthening of reinforced concrete beams with near surface mounted carbon fiber-reinforced polymer. *Buildings*, Vol.11, No. 11, PP. 563.
- [19] Abdo, A., Ahmed, S., Selim, M., & Sharaky, I. A. (2023). Effect of main and NSM reinforcing materials on the behavior of the shear strengthened RC beams with NSM reinforced HSC layers and bars. *Case Studies in Construction Materials*, Vol.18, PP. e02109.
- [20] Bondok, M. H., Debaiky, A. S., & Makhlof, M. H. (2023). Numerical Investigations of GFRC beams strengthened in shear with innovative techniques. *Mansoura Engineering Journal*, Vol.48, No.1, PP2.